9

APPLICATION OF THE DISCRETE FOURIER TRANSFORM METHOD TO PLATE PROBLEMS

C. Y. Shen

9.1   Introduction

Many boundary-value problems in electromagnetic scattering can be solved by using the integral equation technique. In some cases, the resulting differential integral equations will possess the convolution structure, and it would be natural to take advantage of this structure in designing numerical schemes to solve these equations. It is well known that the convolutions can be efficiently handled by Fourier analysis and that, in the case where one of the functions has only finite support, correct convolution values can be computed over any finite region by using only the restriction of the other function over an appropriate chosen set (see Sec. 9.2).

The application of this observation as a means of reducing computer storage in connection with calculating potentials was studied by a number of people in the late 1960's, including Hockney [1], who published his results in 1969. Hockney also pointed out in his paper that the fast Fourier transform (FFT) algorithm can be used to reduce the number of arithmetic operations. In the early1970's, Bojarski [2,3] used this observation to develop independently a numerical technique, called the k–space method, to solve the integral equations arising from elec-

tromagnetic scattering theory. The principal advantage of the k–space method (or, for that matter, any other transform domain methods mentioned later) over that of the Method of Moments (MOM) is its ability to reduce computer memory requirements and to be capable of saving arithmetic operations. In the late 1970's and early 1980's, Mittra and his co-workers [4,5,6] studied a method, called the Spectral Iterative Technique (SIT), which also uses the Fourier analysis to solve scattering problems. However, in those early years, both of these methods had to struggle with the convergence problem of the iterative method used to solve the corresponding discrete equations. A very detailed comparison of the SIT with the MOM (and, to some extent, with the k-space method) can be found in an excellent article by Peterson [7]. Although the Conjugate Gradient Method (CGM) was introduced by Hestenes and Stiefel in 1952, it was not until the mid-1980's that it was made popular for electromagnetic computations by researchers such as Sarkar [8] and van den Berg [9]. The CGM was incorporated into the k-space method as an iterative scheme at the end of 1984. Also, during that same time frame, various versions of still another transform domain technique, called Conjugate Gradient–FFT method (CG-FFT), began to appear in the literature [10,11].

The Discrete Fourier Transform Method (DFTM) was introduced by Shen et al. [12] in the fall of 1985. While it uses the same treatment of the convolution integral as the k-space method, it differs from the k-space or other similar methods such as CG-FFT and SIT in the treatment of differential operators. For the DFTM, the differential operators are left outside the convolution integral and approximated by the appropriate finite difference operators. The finite difference operators are subsequently computed in the discrete Fourier transform space. The use of finite difference formulas in connection with solving the Electric Field Integral Equation (EFIE) has been discussed in the past by Harrington [13], Wilton and Butler [14,15], Hurst and Mittra [16], and others. However, finite difference operators have not previously attracted widespread interest in applications for solving the EFIE, certainly not in the manner as described in the DFTM.

It was shown in [12] that (1) by first casting the differential-integral equation into a periodic form, (2) by approximating the derivatives with the appropriate finite difference operators and by computing them in the discrete transform space, and (3) by using an iterative method such as the CGM to solve the resulting discrete operator equation, the

result will be a simple, accurate, and efficient algorithm to solve the EFIE for a certain class of scattering problems. Perhaps even more important, the present algorithm provides the most natural way in which the discrete Fourier analysis can be applied numerically to solve the differential-integral equations of convolution type. The purpose of the present chapter is to demonstrate that the DFTM, when applied to plate problems, will give accurate Radar Cross Section (RCS) predictions at all times.

9.2 Numerical Formulation

Consider a metallic plate S of arbitrary shape situated in the xy-plane as shown in Fig. 9.1 and illuminated by an incident plane wave $\underline{E}^i$. The incident angles and the polarization angle indicated in Fig. 9.1 are used throughout this paper. The integral equation which characterizes the scattering from such an object is given by

$$(\overline{\overline{I}} + \frac{1}{k^2}\nabla\nabla)\cdot\int_S\int G(\underline{x} - \underline{y})\underline{J}(\underline{y})dS(\underline{y}) = \underline{E}_t^i(\underline{x}), \quad \underline{x}\in S \quad (1)$$

where $G(\underline{x}) = e^{ik|\underline{x}|}/4\pi|\underline{x}|$ is the restriction of the 3-dimensional free space Green's function to the xy-plane, $\nabla = \frac{\partial}{\partial x}\hat{i} + \frac{\partial}{\partial y}\hat{j}$, k the wavenumber, $\underline{E}_t^i(\underline{x})$ the component of the incident field in the xy-plane, and $\underline{J}$ the induced surface current in S which also contains a normalization factor kZ/i involving the intrinsic impedance Z of free space. In the component form, (1) becomes

$$\begin{bmatrix} 1 + \frac{1}{k^2}\frac{\partial}{\partial x^2} & \frac{1}{k^2}\frac{\partial^2}{\partial x\partial y} \\ \frac{1}{k^2}\frac{\partial^2}{\partial x\partial y} & 1 + \frac{1}{k^2}\frac{\partial^2}{\partial y^2} \end{bmatrix}\begin{bmatrix} \int_S\int G(\underline{x} - \underline{y})J_x(\underline{y})dS(\underline{y}) \\ \int_S\int G(\underline{x} - \underline{y})J_y(\underline{y})dS(\underline{y}) \end{bmatrix} = \begin{bmatrix} E_x^i(\underline{x}) \\ E_y^i(\underline{x}) \end{bmatrix}$$
$$(2)$$
$$x \in S$$

In the case where a resistive card is attached to the plate, an extra term of $R(\underline{x})\frac{i}{kZ}\underline{J}(\underline{x})$ must be added to the left-hand side of (1), where $R(\underline{x})$ denotes the resistivity distribution of the card.

Let S be placed in the first quadrant as shown by Fig. 9.2 and let U denote its support function. The first integral in (2) can be written as a 2-dimensional convolution integral

$$\int_{-\infty}^{\infty}\int G(x_1 - y_1, x_2 - y_2)UJ_x(y_1, y_2)dS(y_1, y_2) \quad (3)$$

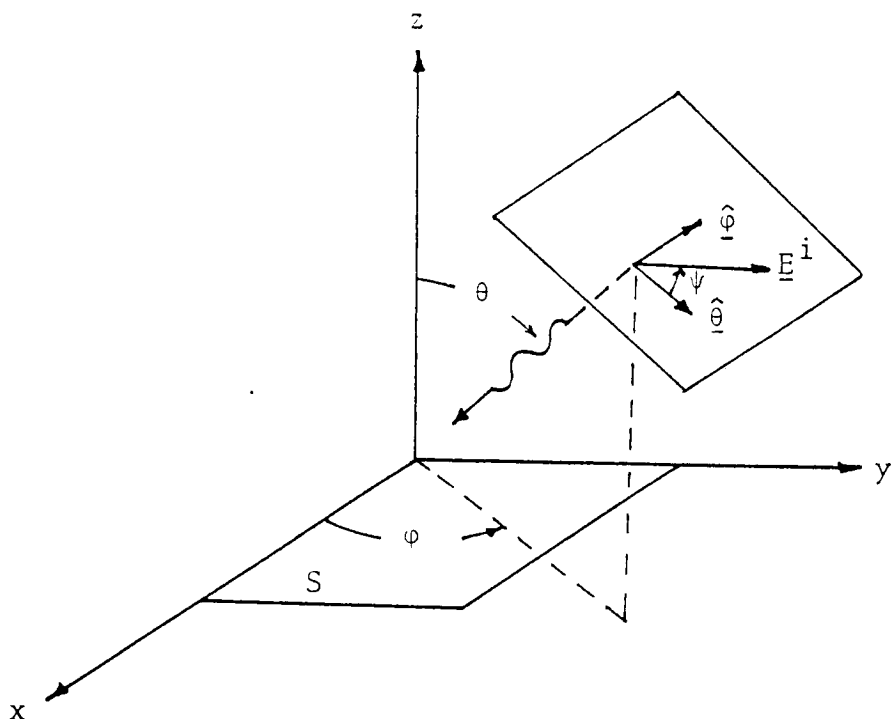**Figure 9.1 The geometry of the plate with respect to the incident field.**

and the same holds true for the second integral. Since UJ_x is a function with finite support, it is easy to see that in order to compute the convolution integral over S, it is not necessary to use all the information about the function G. In fact, only the part of G over the set D, which is twice the size of S (see Fig. 9.2, and also [1], Fig. 9.12), is needed. In other words, if $G_{|D}$ and $UJ_{x|D}$ are the restrictions of G and UJ_x to D, then the integral

$$A_1(x_1, x_2) = \int_D \int G_{|D}(x_1 - y_1, x_2 - y_2)UJ_{x|D}(y_1, y_2)dS(y_1, y_2) \quad (4)$$

will have the same values as the convolution integral in (3) over the set S. For conceptual clarity, the above quantity $A_1(x_1, x_2)$ will be periodically extended from D to the entire xy-plane as follows: Let
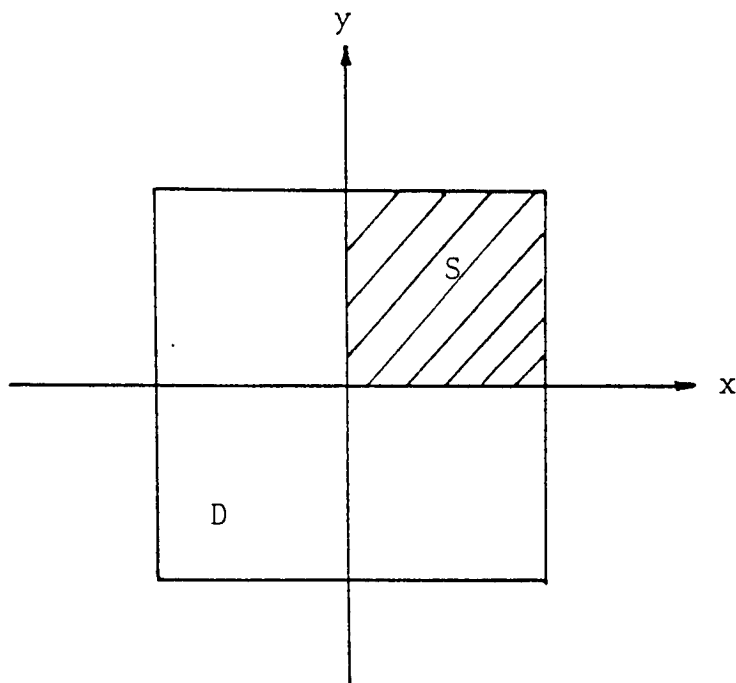
Figure 9.2 Domain Doubling Scheme.

G_P, U_P and $(J_x)_p$ denote the doubly periodical extensions of the functions $G_{|D}$, $U_{|D}$ and $J_{x|D}$ to the xy-plane with D as a unit cell. Then the function

$$(A_1)_p(x_1, x_2) = \int_D \int G_p(x_1 - y_1, x_2 - y_2) U_p(J_x)_p(y_1, y_2) dS(y_1, y_2) \quad (5)$$

where the integration is carried out over the set D or a translation of D, is a periodic extension of A_1. A similar construction can be made for the second integral in (2), and the counter part of $(A_1)_p$ will be denoted by $(A_2)_p$. Now the original differential-integral equation (2) will be replaced by the periodic one,

$$U_p(\underline{x}) \begin{bmatrix} 1 + \frac{1}{k^2} \frac{\partial^2}{\partial x^2} & \frac{1}{k^2} \frac{\partial^2}{\partial x \partial y} \\ \frac{1}{k^2} \frac{\partial^2}{\partial x \partial y} & 1 + \frac{1}{k^2} \frac{\partial^2}{\partial y^2} \end{bmatrix} \begin{bmatrix} \int_D \int G_p(\underline{x} - \underline{y}) U_p(J_x)_p(\underline{y}) dS(\underline{y}) \\ \int_D \int G_p(\underline{x} - \underline{y}) U_p(J_y)_p(\underline{y}) dS(\underline{y}) \end{bmatrix}$$
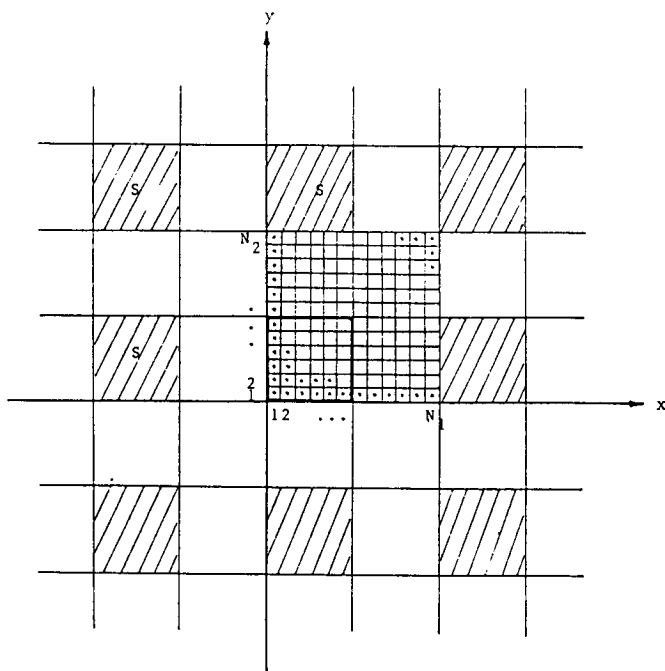
Figure 9.3 A uniform numerical grid for the problem.

$$= \begin{bmatrix} (UE_x^i)_p(\underline{x}) \\ (UE_y^i)_p(\underline{x}) \end{bmatrix} \tag{6}$$

where $(UE_x^i)_p$ and $(UE_y^i)_p$ are the periodic extensions of $(UE_x^i)_{|D}$ and $(UE_y^i)_{|D}$, respectively. This periodic differential-integral equation is defined everywhere except possibly at the boundaries of S and D. It has the same solution over the set S as (2), but has the advantage of a form which can be conveniently analyzed by using the Discrete Fourier Transform Method.

With the introduction of an appropriate uniform grid in the xy-plane as shown in Fig. 9.3, the functions $(A_1)_p$ and $(A_2)_p$ can be approximated by circular discrete convolutions, and the differential operators can be approximated by their corresponding finite difference operators. For example, let Π_{ij} denote the pulse function over the (i,j)-th cell. Then the surface current $U_p(J_x)_p$ can be approximated as a linear combination of pulse functions

$$U_p(J_x)_p(y_1, y_2) \simeq \sum_{i,j} (U_p(J_x)_p)_{ij} \Pi_{ij}(y_1, y_2)$$

$$= \sum_{i,j}(U_p)_{ij}((J_x)_p)_{ij}\Pi_{ij}(y_1, y_2)$$

where $(U_p)_{ij}$ is either 1 or 0 depending on whether the (i,j)–th cell is in S or not, and $((J_x)_p)_{ij}$ are constants. Furthermore,

$$(A_1)_p(m\Delta x, n\Delta y) \simeq \sum_{i,j}(U_p(J_x)_p)_{ij} \int\int G_p(m\Delta x - y_1, n\Delta y - y_2)$$

$$\Pi_{ij}(y_1, y_2)dy_1dy_2$$

$$= \sum_{i,j}(U_p)_{ij}((J_x)_p)_{ij}\mathcal{G}_p(m - i, n - j) \tag{7}$$

where $\mathcal{G}_p(s,t) = \int_{-\frac{\Delta x}{2}}^{\frac{\Delta x}{2}}\int_{-\frac{\Delta y}{2}}^{\frac{\Delta y}{2}} G_p(s\Delta x - y_1, t\Delta y - y_2)dy_1dy_2$ can be evaluated numerically. Again, a similar development can be given for the integral involving the y–component of the surface current.

The discrete convolution sum of (7) can be evaluated by using the discrete convolution theorem as

$$\mathcal{F}^{-1}\tilde{\mathcal{G}}_p[\mathcal{F}U_p(J_x)_p](m,n) \tag{8}$$

where $\mathcal{F}$ is the appropriate discrete Fourier transform, $\mathcal{F}^{-1}$ its inverse, and $\tilde{\mathcal{G}}_p$ the discrete Fourier transform of the sequence $\mathcal{G}_p(s,t)$. Notice that the storage requirement for evaluating the sum (8) is two $N_1 \times N_2$ complex arrays, where $N_1 \times N_2$ is the dimension of the sequence $\mathcal{G}_p(m,n)$, and the number of arithmetic operations required is equal to $O(N_1N_2log(N_1N_2))$ if the Fast Fourier Transform (FFT) algorithm is used. Since $(A_1)_p(m\Delta x, n\Delta y)$(or simply $(A_1)_p(m,n)$) and $(A_2)_p(m,n)$ are periodic sequences, the finite difference formulas approximating various second partial derivatives can be easily applied to them.

As it turns out, these finite difference operators can be most efficiently computed in the discrete Fourier transform domain. Suppose $\frac{\partial^2}{\partial x^2}(A_1)_p(m,n)$ is approximated by the 3–point central difference formula

$$\frac{\Delta^2}{\Delta x^2}(A_1)_p(m,n) =$$

$$\frac{1}{\Delta x^2}[(A_1)_p(m + 1, n) - 2(A_1)_p(m,n) + (A_1)_p(m - 1, n)]$$

It is well known (see, for example, [17,18]) that the discrete Fourier transform of the above formula is given by

$$\frac{\tilde{\Delta}^2}{\Delta x^2}(m,n)(\tilde{A}_1)_p(m,n)$$

with

$$\frac{\tilde{\Delta}^2}{\Delta x^2}(m,n) = \frac{1}{\Delta x^2}\left(cos\frac{2\pi m}{N_1} - 2\right)$$

Calculating finite difference operators in the transform domain requires very little computer storage and does not increase the number of arithmetic operations over that of other similar methods. Also, higher-order approximations such as 5–point central difference formulas can be just as easily carried out as the 3–point formulas. It has been found that the 5–point central difference formulas will provide ample accuracy. The discrete Fourier transforms of 3–point and 5–point difference operators are in the table below. The Fourier transform of the difference formula for the second mixed partial is given by $\frac{\tilde{\Delta}}{\Delta x}\frac{\tilde{\Delta}}{\Delta y}$.

	3−point formula	5−point formula
$\dfrac{\tilde{\Delta}}{\Delta x}$	$\dfrac{i}{\Delta x}sin\dfrac{2\pi m}{N_1}$	$\dfrac{i}{6\Delta x}\left(sin\dfrac{4\pi m}{N_1} + 8\,sin\dfrac{2\pi m}{N_1}\right)$
$\dfrac{\tilde{\Delta}^2}{\Delta x^2}$	$\dfrac{1}{\Delta x^2}\left(2cos\dfrac{2\pi m}{N_1} - 2\right)$	$\dfrac{1}{6\Delta x^2}\left(-cos\dfrac{4\pi m}{N_1} + 16cos\dfrac{2\pi m}{N_1} - 15\right)$

Table 9.1 Fourier transform of difference formulas

As a result of these discussions, it becomes clear that the discretized version of (6) can be expressed as

$$U_p\mathcal{F}^{-1}\tilde{L}_{\Delta\Delta}\tilde{\mathcal{G}}_p\mathcal{F}U_p\underline{I}_p(m,n) = (U\underline{E}_t^i)_p(m,n) \tag{9}$$

where

$$\tilde{L}_{\Delta\Delta} = \begin{bmatrix} 1 + \frac{1}{k^2}\frac{\tilde{\Delta}^2}{\Delta x^2} & \frac{1}{k^2}\frac{\tilde{\Delta}^2}{\Delta x \Delta y} \\ \frac{1}{k^2}\frac{\tilde{\Delta}^2}{\Delta x \Delta y} & 1 + \frac{1}{k^2}\frac{\tilde{\Delta}^2}{\Delta y^2} \end{bmatrix}$$

This discrete operator equation can be solved iteratively by using the CGM. The adjoint operator to

$$L = U_p\mathcal{F}^{-1}\tilde{L}_{\Delta\Delta}\tilde{\mathcal{G}}_p\mathcal{F}U_p$$

is given, in this case, by

$$L^* = U_p \mathcal{F}^{-1} \tilde{L}_{\Delta\Delta} \bar{\tilde{\mathcal{G}}}_p \mathcal{F} U_p$$

where $\bar{\tilde{\mathcal{G}}}_p$ denotes the complex conjugate of $\mathcal{G}_p$.

Finally, a topic closely related to plate problems–the numerical treatment of nonorthogonal corner reflectors–is worthy of mention. The key ingredients involved here are three:

(1)The corner reflector is thought of as two plates. The scattered field radiated by each plate can be calculated by using the DFTM at uniformly spaced points in space.

(2) In order to avoid placing observation points on the intersection of two plates, the uniform grid associated with one plate cannot coincide with that of the other. Thus an interpolation scheme must be introduced in order to calculate the incident scattered field from one plate onto the other. The 4−point bivariate Lagrange interpolation method is carried out in the discrete Fourier transform domain, an approach which makes it extremely simple for the interpolation method to be incorporated in the DFTM.

(3) A simple coordinate transformation can be used to reduce the mathematical treatment of a nonorthogonal corner reflector to that of the much simpler case of an orthogonal corner reflector.

A detailed discussion of the numerical treatment of nonorthogonal corner reflectors can be found in [19], and the techniques introduced in that paper are useful in performing large-scale parallel computations.

9.3   Numerical Results

The calculation of RCS for H−pol grazing sweep $(\theta = \pi/2, \psi = \pi/2, 0 \leq \varphi \leq \pi/4)$ of a $3\lambda \times 3\lambda$ metallic plate is made at 10 GHz, and presented in Fig. 9.4. The experimental result for this case is given in Fig. 9.5. Both results are plotted with the same large scale but not superimposed. In this way they can be easily compared with each other by overlaying one on top of the other and, at the same time, can be conveniently used by others for validation purposes.
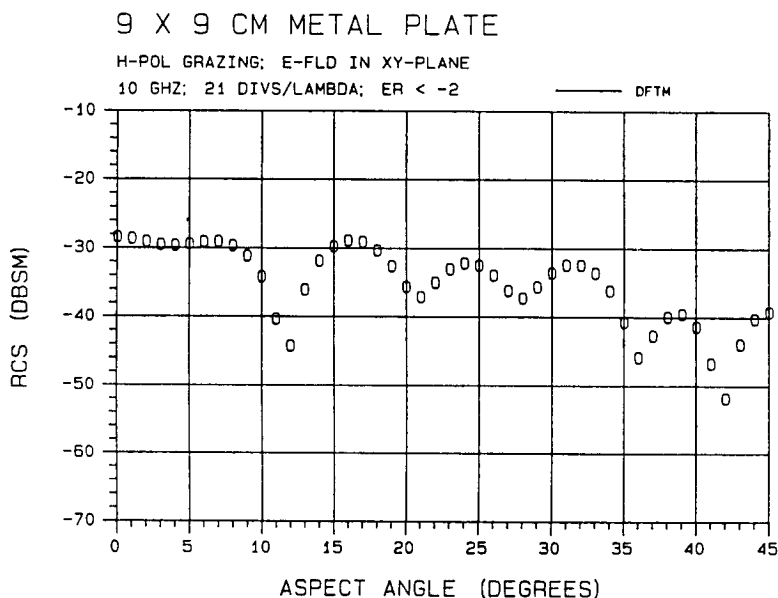
9 X 9 CM METAL PLATE

H-POL GRAZING; E-FLD IN XY-PLANE

10 GHZ; 21 DIVS/LAMBDA; ER < -2 ———— DFTM

Figure 9.4 RCS prediction for the H-pol grazing sweep of $3\lambda \times 3\lambda$ metallic plate.

The prediction for the H-pol grazing sweep of a $5.355\lambda \times 6.773\lambda$ parallelogram-shaped metallic plate at 10 GHz is given in Fig. 9.6. The agreement with the experimental result (not shown) is extremely good.

The RCS for an orthogonal corner reflector made of two $5.6088\lambda \times 5.6088\lambda$ metallic plates has been calculated for the V-pol sweep (the incident E-field is parallel to the folding axis) at 9.4 GHz. The result and its accompanying measurement are presented in Figs. 9.7 and 9.8, respectively.
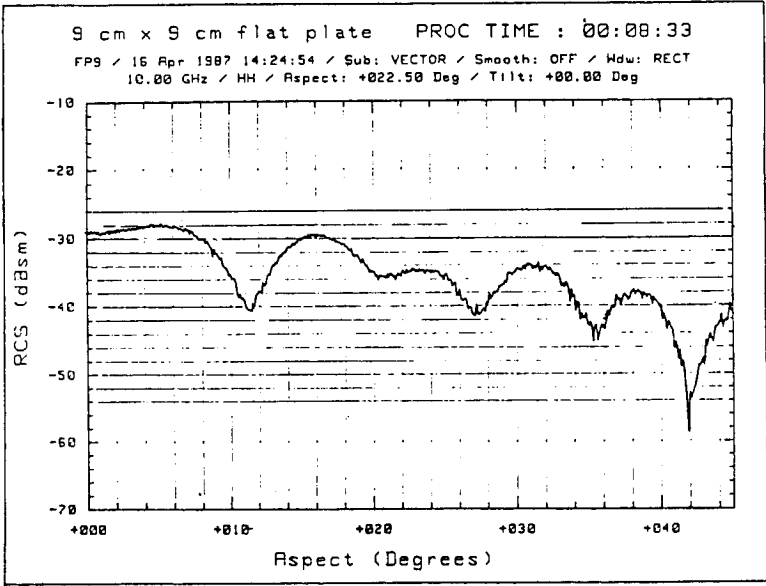
Figure 9.5 Experimental result for the H-pol grazing sweep of a $3\lambda \times 3\lambda$ metallic plate.
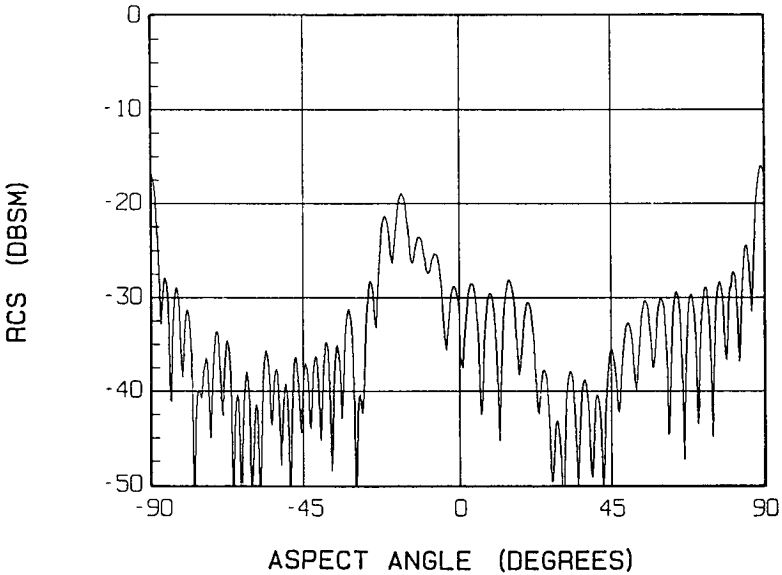

Figure 9.6 RCS prediction for the H-pol grazing sweep of a $5.355\lambda \times 6.773\lambda$ parallelogram-shaped metallic plate (height = 5.08λ).
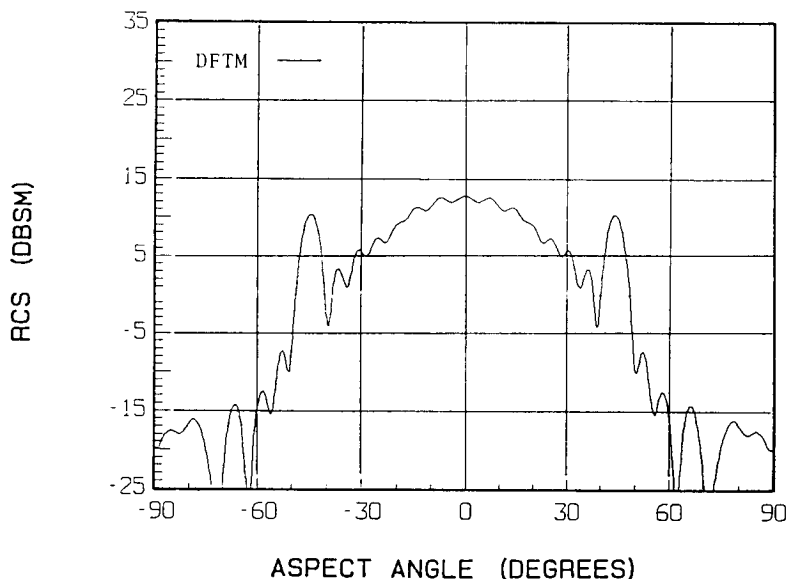
Figure 9.7 The V-pol sweep of a $5.6088\lambda \times 5.6088\lambda$ orthogonal corner reflector.

The similar results for a corner reflector of the same size but with an interior angle of 77 degrees are given in Figs. 9.9 and 9.10. The resolution used in these calculations is 11 divisions per wavelength, which has resulted in approximately 15,000 complex unknowns and 15 megawords memory requirement. The logarithmic root–mean–square error criterion was set at -1.6.

The theoretical study of the low frequency limit is certainly an interesting topic in scattering theory. It is known that when the geometry of a metallic scatterer is not too complicated, the scattered fields will converge to that of the static case as the wavenumber k approaches zero (see [20]). Of course, under the computational environment, the EFIE ceases to provide a correct solution when k becomes too small. A remedy to this problem has been suggested by Mautz and Harrington [21], and their method seems to work very well when applied to a small conducting disk at normal incidence. The DFTM, in its present form and without any modification, is used to calculate the H-pol sweep $(\varphi = 0, \psi = \pi/2, 0 \leq \theta \leq \pi/2)$ for square plates of dimensions as small as $.01\lambda$. When the plate size gets down to $.01\lambda$, the RCS calculation stays flat from normal to grazing incidence, a result which signifies
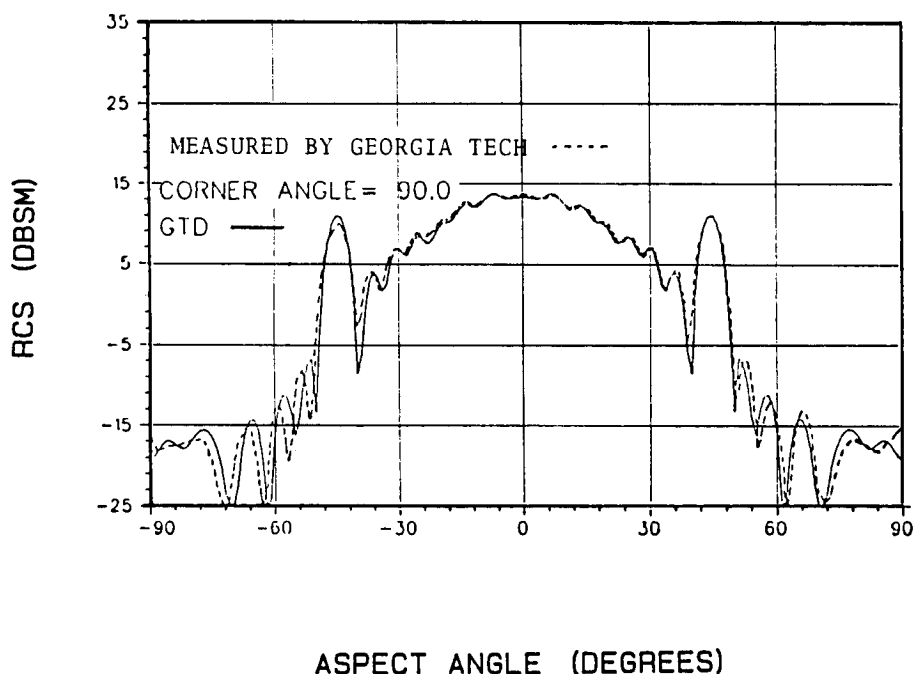
RCS (DBSM)

MEASURED BY GEORGIA TECH ----

CORNER ANGLE = 90.0

GTD ——

ASPECT ANGLE (DEGREES)

Figure 9.8 Measurement of the V-pol sweep of a 5.6088λ × 5.6088λ orthogonal corner reflector.

the breakdown of the method, since the value of the RCS at grazing incidence should be about 3.5 dB higher than that of normal incidence ([22], page 510). However this pattern does prevail, albeit with less than 3.5 dB differential, in the case of a .05λ square plate. This result and also the result of a frequency sweep at normal incidence for a 24″ × 24″ square plate are given in Figs. 9.11 and 9.12, respectively. It should be pointed out that in order to obtain reasonable results at low frequencies, the resolution must be increased to 30 divisions per wavelength or higher.
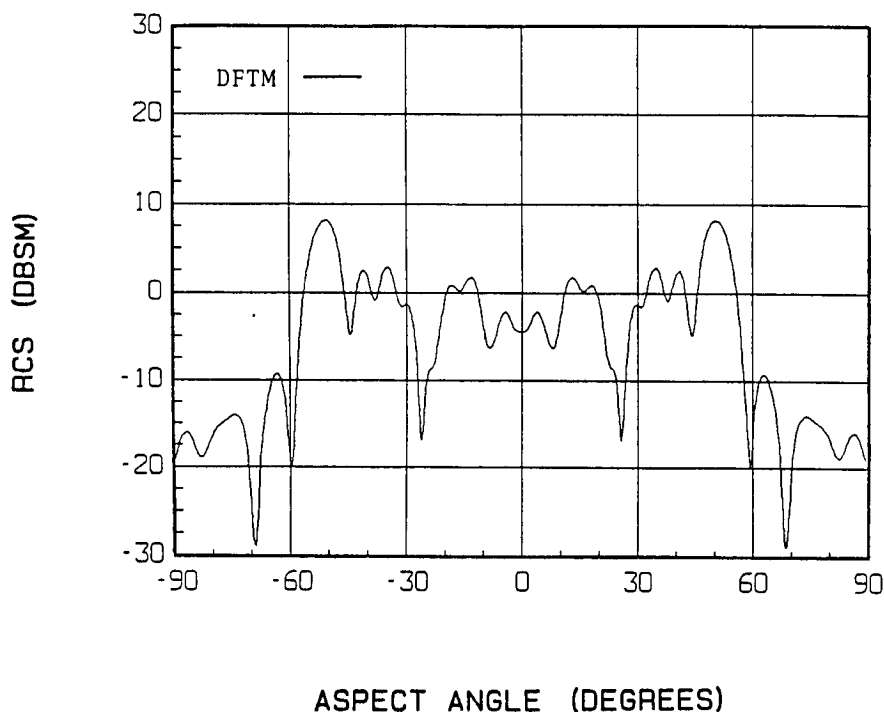
Figure 9.9 The V-pol sweep of a $5.6088\lambda \times 5.6088\lambda$ corner reflector with the interior angle of 77 degrees.

To further test the robustness of the DFTM, the RCS of a narrow plate of dimension $.1\lambda \times 5\lambda$ was compared with that of a 5λ wire. It was found that the H-pol grazing sweep and the V-pol sweep ($\varphi = 0, \psi = 0, 0 \leq \theta \leq \pi/2$) for the plate are very much the same and, furthermore, that they agree well with the corresponding result for the wire. This observation has some practical usefulness in the study of the effects of a finite crack in an infinite ground plane. These results are presented in Figs. 9.13, 9.14, and 9.15.

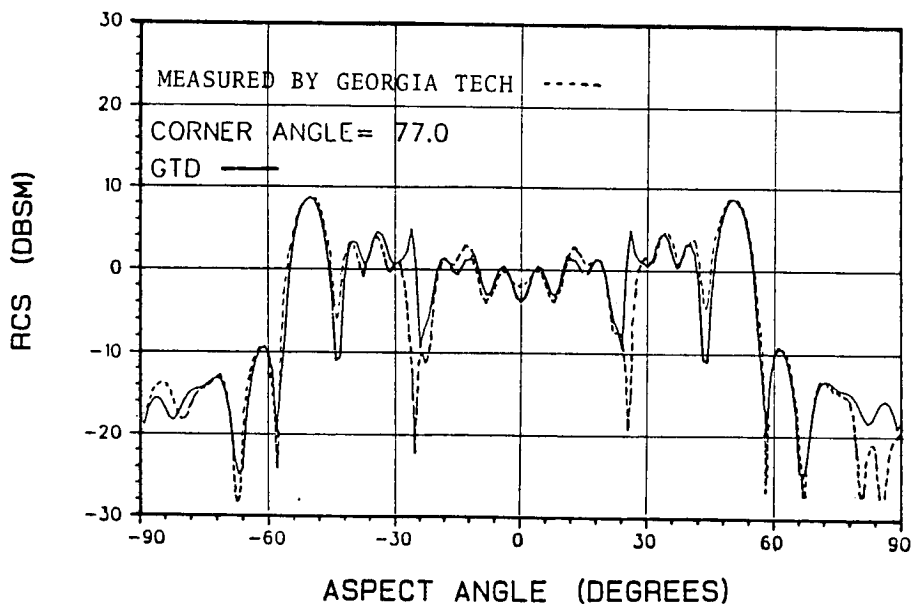Two major weaknesses are associated with the transform domain

Figure 9.10   Measurement of the V-pol sweep of a $5.6088\lambda \times 5.6088\lambda$ corner reflector with the interior angle of 77 degrees.

methods: one of them is the requirement of a uniform grid scheme which will cause a staircase effect at the curved boundary of a scatterer, and the other is the problem of slow convergence often associated with the CGM. For the latter problem, various pre–conditioning schemes have been reported in the literature (see, for example, [23,24,25]). Unfortunately, most of them have worked well only with 1-dimensional problems but failed for higher dimensional problems. However it has been generally observed that smoother basis functions will yield a better condition number for the discrete operator equation and, consequently, give a better rate of convergence. The result given by Fig. 9.16 shows that when the rooftop functions instead of the usual pulse functions were used as the expansion functions, the rate of convergence of the CGM would improve by a factor of two. However, rooftop functions are difficult to use when the geometry of the scatterer is different from that of a rectangle. For general purposes, pulse basis functions together with pointwise collocation is the best combination to be used with the DFTM.

As a demonstration of the ability of the DFTM to handle very large-scale computations, the RCS of a square plate of $20.48\lambda \times 203.2\lambda$
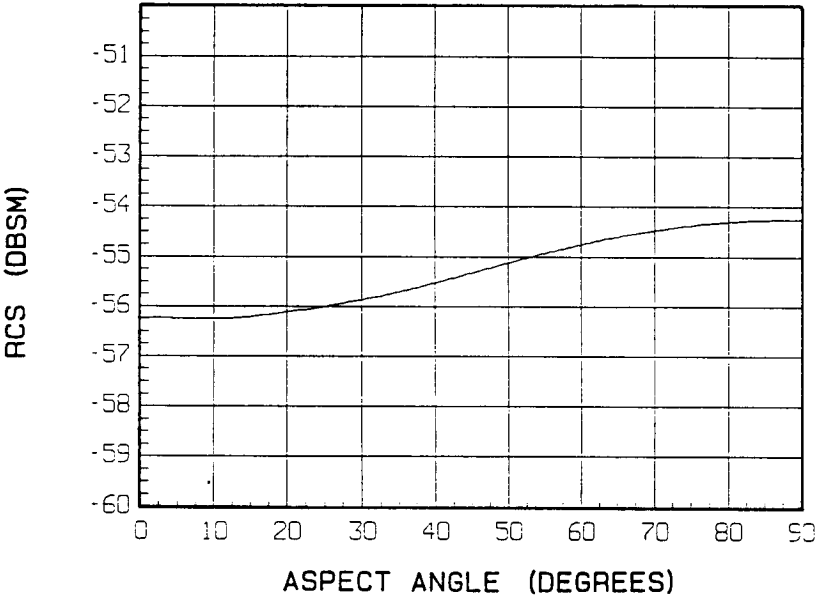
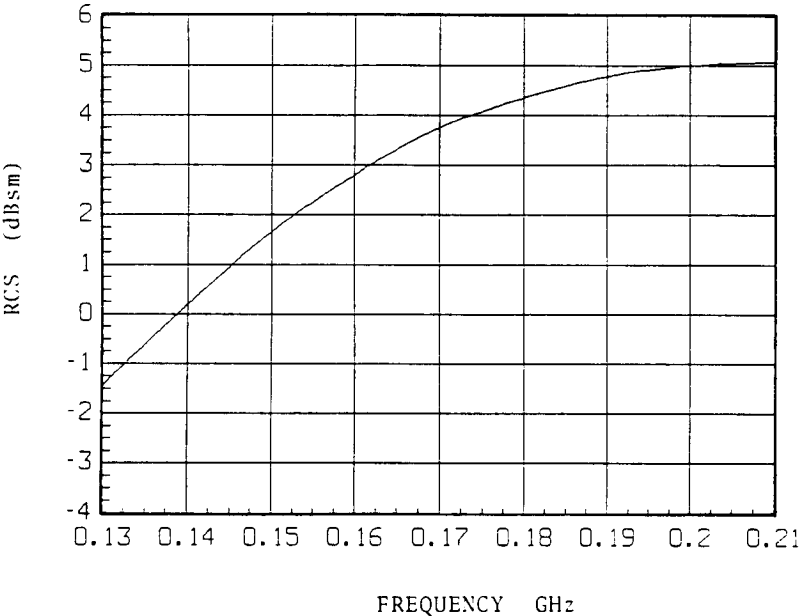**Figure 9.11   H-pol sweep for a .05λ × .05λ metallic plate.**

FREQUENCY   GHz

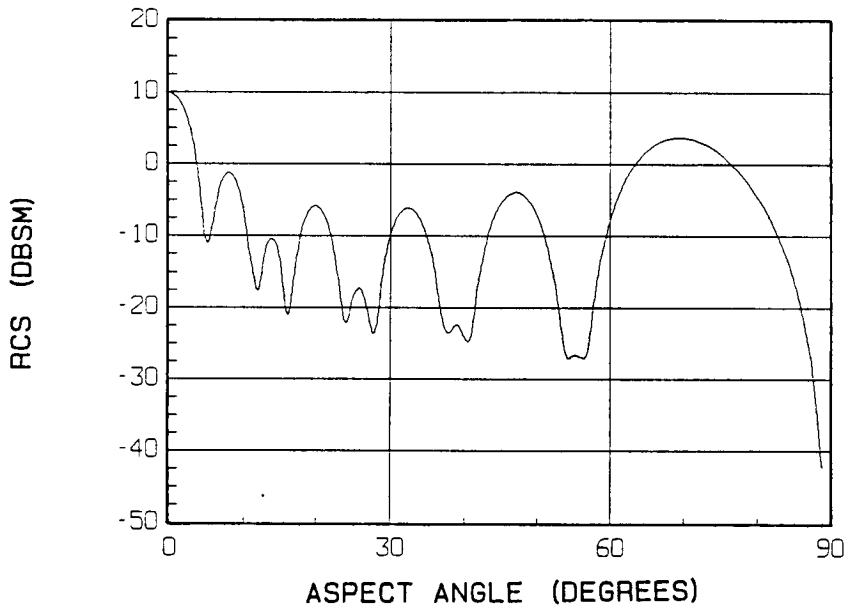**Figure 9.12   Low frequency sweep for a 24″ × 24″ metallic plate.**

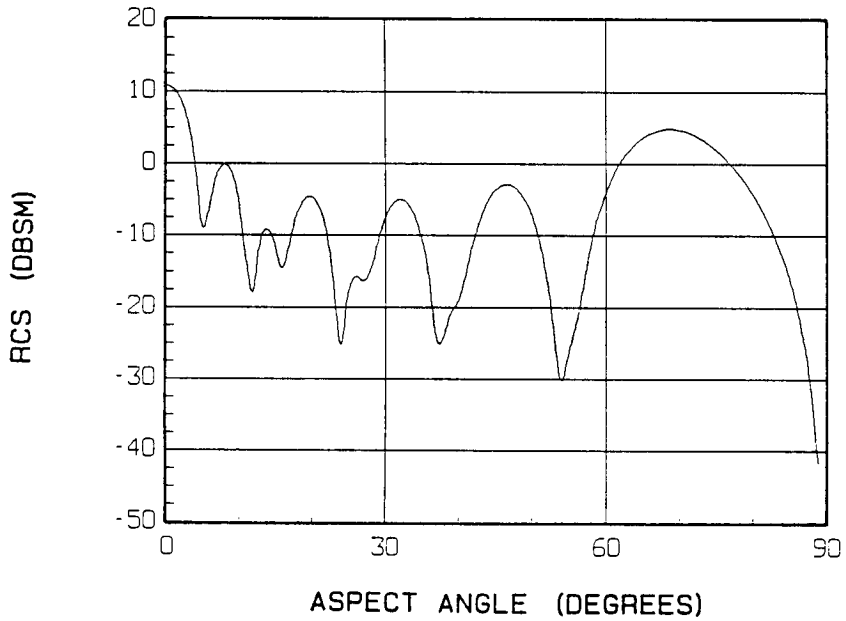**Figure 9.13 H-pol grazing sweep for a narrow metallic plate of $.1\lambda \times 5\lambda$.**

Figure 9.14 V-pol sweep for a narrow metallic plate of $.1\lambda \times 5\lambda$.
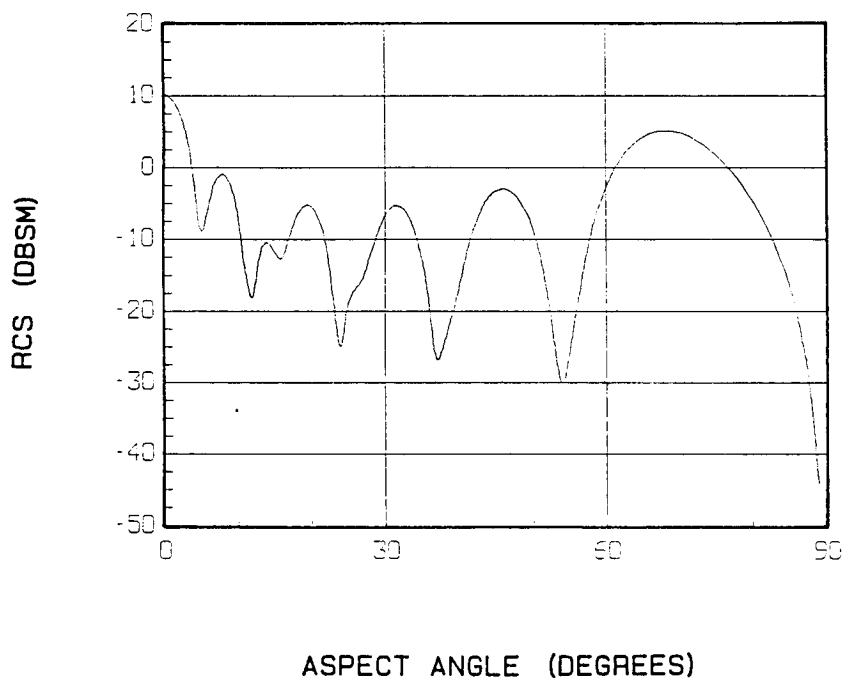
ASPECT ANGLE (DEGREES)

Figure 9.15   Elevation sweep $(0 \leq \theta \leq \pi/2)$ **for a** 5λ **thin wire of radius** $1/50\lambda$.

at normal incidence is computed on Cray Y-MP with 128 megawords memory, 8 processors, and 5 nanoseconds clock cycle. At 10 divisions per wavelength, this problem generates 1.04 million of complex unknowns, and at 20 divisions per wavelength, 4.2 million of complex unknowns. At 20 divisions per wavelength, it takes 45.48 CPU seconds (5.7 seconds by wallclock) to complete one iteration and 30 iterations to reach the logarithmic root–mean–square error of -1.6. The predicted RCS is 86.81 dBsm (at either 10 or 20 divisions per wavelength) as compared to 86.83 dBsm by using the Physical Optics method. The computer memory requirement at 20 divisions per wavelength is 114.2 megawords. There do not appear to be any corruptions due to round-off errors on the calculations.
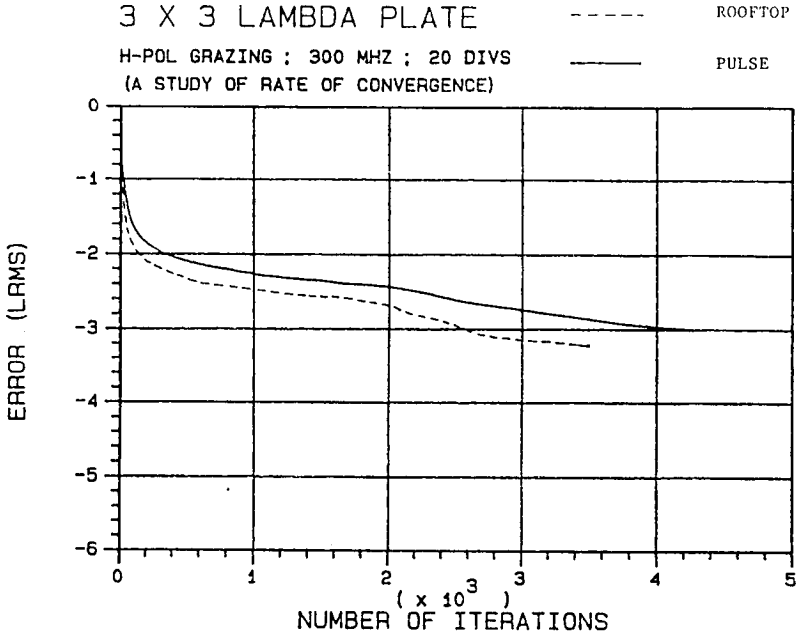
Figure 9.16 Comparison of the rate of convergence of the CGM between two different expansion functions (pulse vs. rooftop).

9.4   Conclusion

Despite the recent surge of interest in using the finite difference or finite element method to solve electromagnetic scattering problems, the integral equation method will still prove to be a powerful and indispensable tool in dealing with a variety of scattering problems. As in any field of scientific computing, it is difficult to claim a particular method is superior to the rest, or is capable of solving all the interesting problems in that field. Most likely, each of these techniques is suitable for a particular type of problem; and perhaps only through a combination of these different methods does hope exist to solve a complicated, real-world problem.

When a differential-integral equation of convolution type is defined over a region which can be modeled accurately by a piecewise uniform grid, the DFTM proves to be a powerful tool in solving such problems. As demonstrated in this chapter, the DFTM will produce accurate solutions when it is applied to a variety of plate problems. In fact, it is generally capable of solving electrically large problems on computers with very limited capabilities.

The Discrete Fourier Transform Method is accurate, simple to program, and computationally efficient. Some of the results that have been reported here do not seem to have appeared elsewhere in the open literature. Besides plate problems, there are many other important applications of the present method–for example, the study of finite frequency selective surfaces, microstrip antennas, and corner reflectors. Without any doubt, the DFTM should play a significant role in electromagnetic computations.

References

[1] Hockney, R. W., "The potential calculation and some applications," *Methods in Computational Physics*, **9**, N. Y. and London: Academic Press Inc, 1969.

[2] Bojarski, N. N., "K-space formulation of the electromagnetic scattering problems," Tech. Rep. AFAL-TR-71-75, Air Force Avionics Lab., Wright-Patterson Air Force Base, Ohio, March, 1971.

[3] Bojarski, N. N., "K-space formulation of electromagnetic scattering problems," *Technical Report*, Defense Technical Information Center, 1972.

[4] Ko, W. L., and R. Mittra, "A new approach based on a combination of integral equation and asymptotic techniques for solving electromagnetic scattering problems," *IEEE Trans. Antennas Propagat.*, **AP-25**, 187–197, March, 1977.

[5] Tsao, C. H., and R. Mittra, "A spectral iterative technique for analyzing scattering from frequency selective surfaces," *IEEE Trans. Antennas Propagat.*, **AP-30**, 303–308, March, 1982.

[6] Kastner, R., and R. Mittra, "A special iterative technique for analyzing scattering from arbitrary bodies, Part I: Cylindrical scatterers with E-wave incidence," *IEEE Trans. Antennas Propagat.*, **AP-31**, 535–537, May, 1983.

[7] Peterson, A. F., "An analysis of the spectral iterative technique for electromagnetic scattering from individual and periodic structures," *Electromagnetics*, **6**, 255–276, 1986.

[8] Sarkar, T. K., and S. M. Rao, "The application of conjugate gradient method for the solution of electromagnetic scattering from arbitrary oriented wire antenna," *IEEE Trans. Antennas Propagat.*, **32**, 398–403, April, 1984.

[9] van den Berg, P. M., "Iterative computational techniques in scattering based upon the integrated square error criterion," *IEEE Trans. Antennas Propagat.*, **AP-32**, 10, 1063–1071, October, 1984.

[10] Sarkar, T. K., E. Arvas, and S. M. Rao, "Application of FFT and the conjugate gradient method for the solution of electromagnetic radiation from electrically large and small conducting bodies," *IEEE Trans. Antennas Propagat.*, **AP-34**, 5, 635–640, May, 1986.

[11] Borup, D., and O. P. Gandhi, "Fast Fourier transform method for calculation of SAR distribution in finely discretized inhomogeneous models of biological bodies," *IEEE Trans. Microwave Theory Tech.*, **MTT-32**, April, 1984.

[12] Shen, C. Y., K. J. Glover, M. I. Sancer, and A. D. Varvatsis, "The discrete Fourier transform method of solving differential-integral equations in scattering theory," *IEEE Trans. Antennas Propagat.*, **AP-37**, 8, 1032–1041, August, 1989.

[13] Harrington, R. F., *Field computation by moment methods*, New York: Macmillan, 1968.

[14] Butler, C. M., and D. R. Wilton, "Analysis of various numerical techniques applied to thin-wire scatterers," *IEEE Trans. Antennas Propagat.*, 534–540, July, 1975.

[15] Wilton, D. R., and C. M. Butler, "Effective methods for solving integral and integral-differential equations," *Electromagnetics*, 1, 3, July–Sept., 1981.

[16] Hurst, M., and R. Mittra, "Scattering center analysis for Radar Cross Section modification," *Numerical techniques for RCS computation and scattering center approach to RCS modeling*, 4, SCEEE Publication, 1987.

[17] Weaver, H. J., *Applications of discrete and continuous Fourier analysis*, New York: John Wiley & Sons, 1983.

[18] Vichnevetsky, R., and J. B. Bowles, "Fourier analysis of numerical approximations of hyperbolic equtions," *SIAM Pub.*, 1982.

[19] Shen, C. Y., "Application of the discrete Fourier transform method to nonorthogonal dihedral reflectors," *IEEE Trans. Antennas Propagat.*, December, 1990.

[20] Colton, D., and R. Kress, *Integral equation methods in scattering theory*, New York: John Wiley & Sons, 1983.

[21] Mautz, J. R., and R. F. Harrington, "An E-field solution for a conducting surface small or comparable to the wavelength," *IEEE Trans. Antennas Propagat.*, **AP-32**, 4, 330–339, April, 1984.

[22] Ruck, G. T., D. E. Barrick, W. D. Stuart, and C. K. Krichbaum, *Radar Cross Section Handbook*, New York–London: Plenum Press, 1970.

[23] Chen, R. H., and G. Strang, "The asymptotic Toeplitz–circulant eigenvalue problems," *SIAM J. on Sci & Stats. Computing*, 1989.

[24] van den Berg, P. M., and R. E. Kleinman, "The conjugate gradient spectral iterative technique for planar structures," *IEEE Trans. Antennas Propagat.*, **36**, 10, 1418–1423, Oct., 1988.

[25] Kas, A., and E. L. Yip, "Preconditioned conjugate gradient methods for solving electromagnetic problems," *IEEE Trans. Antennas Propagat.*, **35**, 2, 147–152, Feb., 1987.